

PARTITION OF HEAT FLUXES AND STRUCTURES RELATED TO A JET STREAM

by I. Gültepe

NASA, Goddard Space Flight Center, Code 913, Greenbelt, MD 20771

Abstract

Aircraft data collected during the First International Satellite Cloud Climatology Project (ISCCP) Regional Experiment (FIRE) which took place over Wisconsin were used to explain updraft events and heat fluxes in case of a jet stream cirrus cloud. Aircraft measurements for the 31 October 1986 case are used in the calculations. Flight patterns used to gather the data were: (1) step up, (2) the spiral descent, and (3) sloping ascent. The cirrus on the 31 October case formed because of large scale moisture advection in the sloping surfaces, and shear and buoyancy convection played further role for cloud development. The goal of this study is to estimate the size of the convective cells and fluxes in the jet stream cirrus. Results showed that both turbulence and gravity wave activity were found in the region of strong shear. A strong inversion layer at about 8.7 km divided the cloud into two regions: 1) a relatively unstable layer above where turbulence and gravity wave activity were observed and 2) a stable layer below where mainly gravity waves ($\leq \lambda=40$ km) were observed. Size of the convective cells were about 3 km.

1. Introduction

Cirrus clouds because of their complex physical and

thermodynamical structure play an important role for atmospheric processes. Their formation, development, and decay are strongly related to dynamical, thermodynamical, and radiative changes in the dry or moist environment, depending on scale. Cirrus associated with jet streams may cover large areas (about 650 km across and 1000's km along horizontal wind, Conover, 1960) where strong dynamical, physical, and radiative processes are important. In addition to stratiform cirrus, embedded or separate cells were also observed in the jet stream clouds (Nakagawa and Frenzen, 1954).

Convective and meso-scales structures (e.g., turbulence and waves) in cirrus clouds can be very important for mass, heat and momentum transfer, and cloud history (Gültepe and Starr, 1992). They showed that meso-scale convective cells can have a size up to 10 km. Large scale processes also play a very crucial role in cirrus formation. Even a few cm s⁻¹ vertical velocity may generate cirrus cloud in a environment where the relative humidity with respect to ice is high (Schaefer, 1955; Starr and Wylie, 1990).

Structures in jet stream cirrus are not known properly. On the other hand, there are several significant studies about structures of boundary layer clouds, indi-

cating convection (LeMone, 1983; Greenhut and Khalsa, 1982), and turbulence and gravity waves (Holt and Raman, 1992; Shao et al., 1991). But, because of measurement difficulties, there are limited studies related to cirrus clouds.

The main goal of this study is to understand dynamical and thermodynamical structure of a jet stream cirrus cloud. Data used in this study were obtained from the First International Satellite Cloud Climatology Project (ISCCP) Regional Experiment (FIRE I) field project which took place over Wisconsin region.

2. Aircraft Measurements

Data for this study were collected by the NCAR King Air during the FIRE experiment on 31 October 1986 over Wisconsin. The NCAR King Air gathered data in three different flight patterns: (1) Spiral descent, (2) Step-up, and (3) Sloping ascent.

In the spiral flight pattern, the aircraft drifted with the wind while descending at a fairly constant rate of 2.8 ms^{-1} . This type of flight pattern is useful for understanding of cloud structure in the vertical. In the step-up flight pattern, the aircraft collected data along constant altitude flight legs. The vertical separation between legs was about 300 m

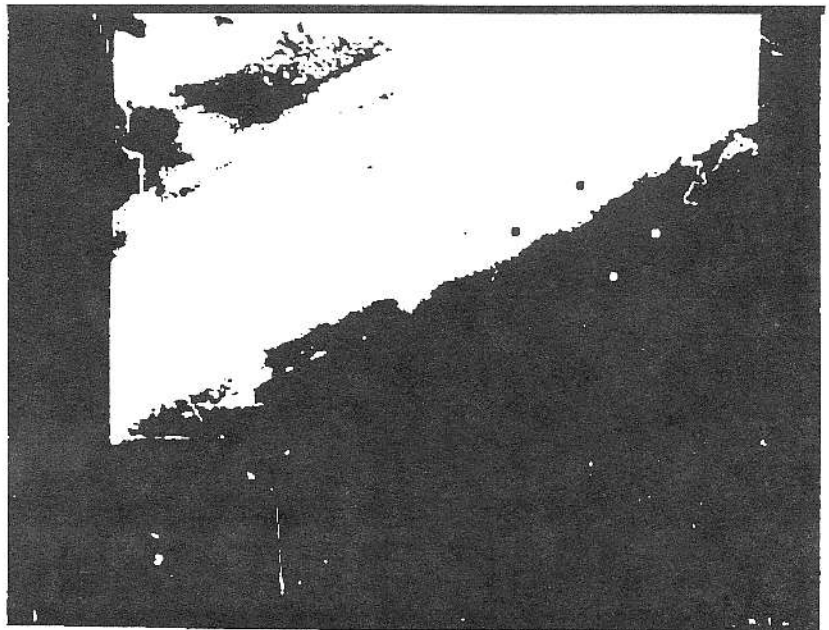


Figure 2. GOES satellite imagery at 18:01 UTC on 31 October 1986. Squares represent the significant areas for the data collection.

and the aircraft heading was parallel to the jet stream. Figure 1 shows the flight pattern that was used over the time period from 15:28 to 17:28 UTC. Table 1 the altitudes for the constant altitude flight legs and type of sounding. Time period for each constant altitude flight leg is about 300 seconds and for soundings it is about 15 minutes.

The measurements used in this study were described by Gültepe et al. (1990). The basic measurements are pressure, temperature and dewpoint, wind components, particle size, shape, and concentration. The sampling rate of the measurements was 1 Hz. In the analysis, data collected when sharp changes occurred (in the pitch, roll, and heading) were removed because of large bias in the measurements.

Environmental conditions on 31 October 1986 case were suitable for cirrus formation. Moisture flow from SW to NE was significant. Shear generated instability obtained from aircraft measurements was also found. Cirrus clouds streaming from SW to NE parallel to jet core is shown in the GOES satellite IR imagery (Figure 2) taken at 18:01 UTC on 31 October 1986. In this figure, Wisconsin region indicated with squares is seen nearby Michigan Lake where horizontal wind speeds reached up to 35 ms^{-1} .

3. Calculation Techniques

Analysis technique used here is based on conditional mean distribution and the joint frequency distribution (Grossman,

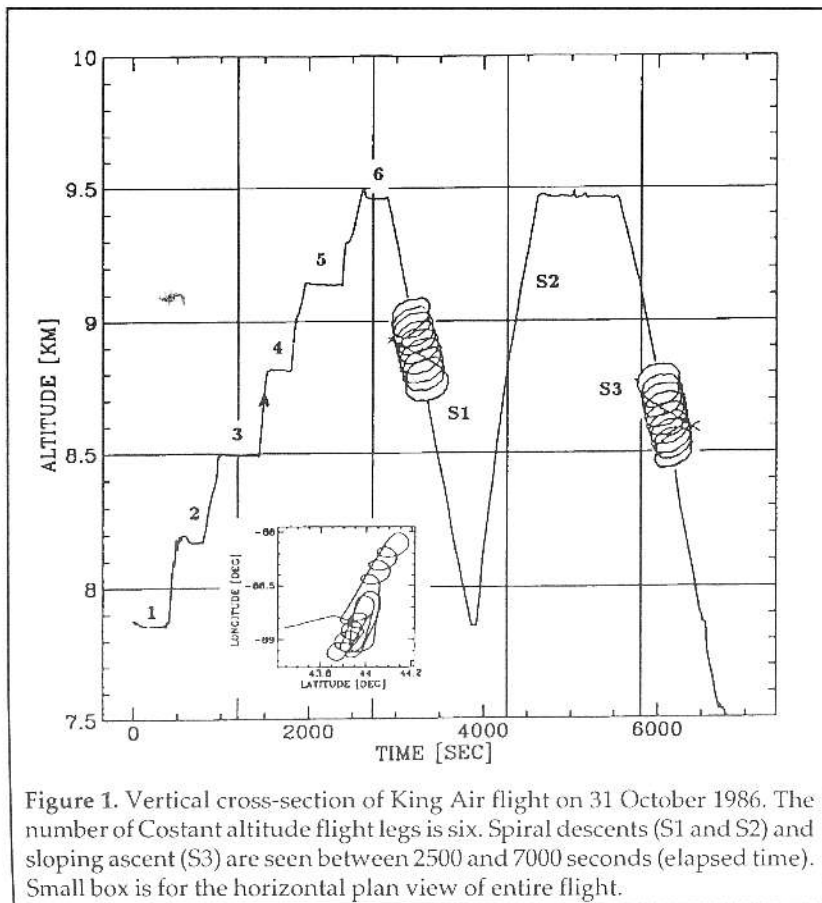


Figure 1. Vertical cross-section of King Air flight on 31 October 1986. The number of Constant altitude flight legs is six. Spiral descents (S1 and S2) and sloping ascent (S3) are seen between 2500 and 7000 seconds (elapsed time). Small box is for the horizontal plan view of entire flight.

Leg	Altitude [km]
1	7.75
2	8.17
3	8.48
4	8.80
5	9.15
6	9.45
Sounding	Type
s1	Lagrangian descent
s2	Sloping ascent
s3	Lagrangian descent

Table 1. Constant altitude flight legs and type of sounding for 31 October 1986 during FIRE I field project.

1984). The value of vertical velocity and saturated potential temperature fluctuations are obtained from time series of these parameters. First, they are de-trended. Second, their means are removed. Then, the fluctuations of w and θ_e are obtained to calculate heat flux. After that, fluxes based on their signs are discussed. The leg averaged heat fluxes (and others) are calculated as:

$$\overline{w'\theta'_e} = \frac{1}{n} \sum w'\theta'_e, \quad (1)$$

where n is the number of data points in the leg. Prime signifies the fluctuations.

According to Grossman (1982), using sign and magnitude of fluctuations, fluxes can be interpreted as cell core, lateral entrainment to cell, and lateral detrainment from the cell. Table 2 shows the partition of the each feature. In case of large fluctuations of both w (+) and θ_e (+), cell core moves upward. If both w (-) and θ_e (-) have large values, the cell moves downward. When w is small and θ_e is large, flux is hypothesized as direct flux associated with small-scale local compensation flow around the cell. Small-scale mixing processes are connected to indirect fluxes. The important combination of

w'	T'	w'	T'	Interpretation	Process
+	-	large	large	small scale	up-cell LE or down-cell LD
+	-	small	small	small scale	C within down-cell or M from top of cell
+	+	large	large	large scale	up-cell core
+	+	small	large	small scale	down-cell local compensation flow
-	+	large	large	small scale	up-cell LD or down-cell LE
-	-	small	small	small scale	C within up-cell, M from top of cell
-	-	large	large	large scale	down-cell core
-	-	small	large	small scale	up-cell local compensation flow

Table 2. Partition of heat fluxes and physical interpretation of statistical results (adapted from Grossman, 1984).

w' and θ_e' with opposite signs and large values indicates lateral entrainment and detrainment which are dominant mixing process. In case of flight legs close to cloud top and cloud base, large values of $w'\theta_e'$ (-+ or +-) likely indicate cloud top or base mixing values.

Structures (e.g., turbulence, convective cells, and gravity waves) in the cirrus are analyzed by using time series and profiles of aircraft measurements. Spectral analysis technique is not used because of short flight legs and sampling rate (i.e., 1Hz).

Greenhut and Khalsa (1982) calculated draft threshold from time series of w' . If w' is larger than its threshold value, it is defined as a convective cell. Threshold for an updraft cell is simply given as

$$w_{th}^+ = \alpha_{trs} \sigma_w^+ \quad (2)$$

and for downdrafts is

$$w_{th}^- = \alpha_{trs} \sigma_w^- \quad (3)$$

where

$$\alpha_{trs} = \frac{\sigma^+}{\sigma^-} \quad (4)$$

The (+) and (-) in the above equations signify the updraft and downdraft, respectively. The σ^+ and σ^- represent standard deviations for positive and negative fluctuations of w , respectively. The σ_{trs} is the threshold multiplier. Convective scale updrafts in the planetary boundary layer are defined if the length of cell is less than 6 km (Lemone, 1983) and mesoscale updrafts with cell sizes larger than 6 km.

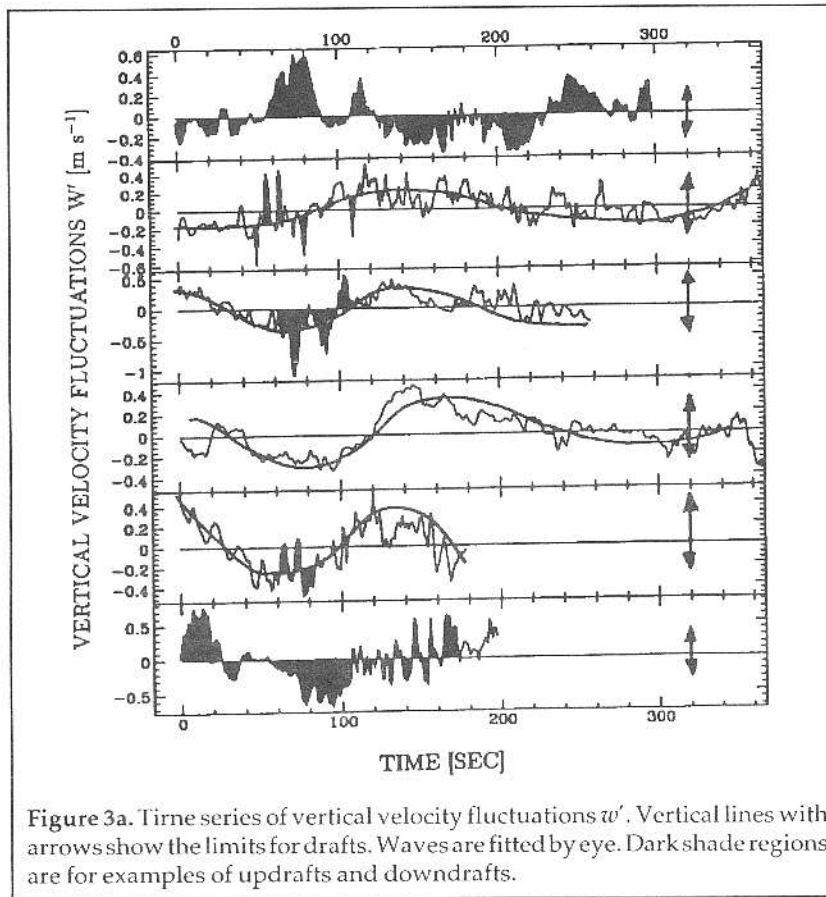
4. Results

The results from the analysis of time series, and sizes of cells and gravity wave characteristics will be summarized in this section.

4.1 Time series analysis

Time series of measurements are used for defining the scale of the dominant phenomena (e.g., turbulence or gravity waves). Because of low data sampling rate (i.e., 1 Hz) and short flight legs, spectral analysis is not used for specifying the region of turbulence or wave phenomena.

Time series of w' at each flight leg are shown in Figure 3. The lowest box belongs the flight leg 1. Wave like structure is clearly seen along legs 2, 3, 4, and 5. The apparent wave length becomes larger on the upper flight legs where environment is relatively unstable. Significant updrafts and downdrafts are found along flight legs 1, 2, and 6. In leg 6, this may possibly be attributed to entrainment of dry and cold air from above. A change in w of about 1 ms^{-1} over 1 km distance in the leg 1 indicates that relatively strong turbulent heat, moisture, and momentum transfer which likely play an important role in development of this cirrus cloud system. for cirrus development. On the other



hand, turbulent fluctuations are found to be smaller on the mid-level flight legs. Table 3 shows the statistics of the dominant processes seen in in time series of w' . Sizes of the cells estimated from time series of w' and aircraft true airspeed ($\approx 100 \text{ ms}^{-1}$) are found to be less than 3 km.

4.2 Aircraft soundings

The soundings from the aircraft spiral descents and a sloping ascent maneuver are used to understand cirrus structure in the vertical and support the findings seen in the time series.

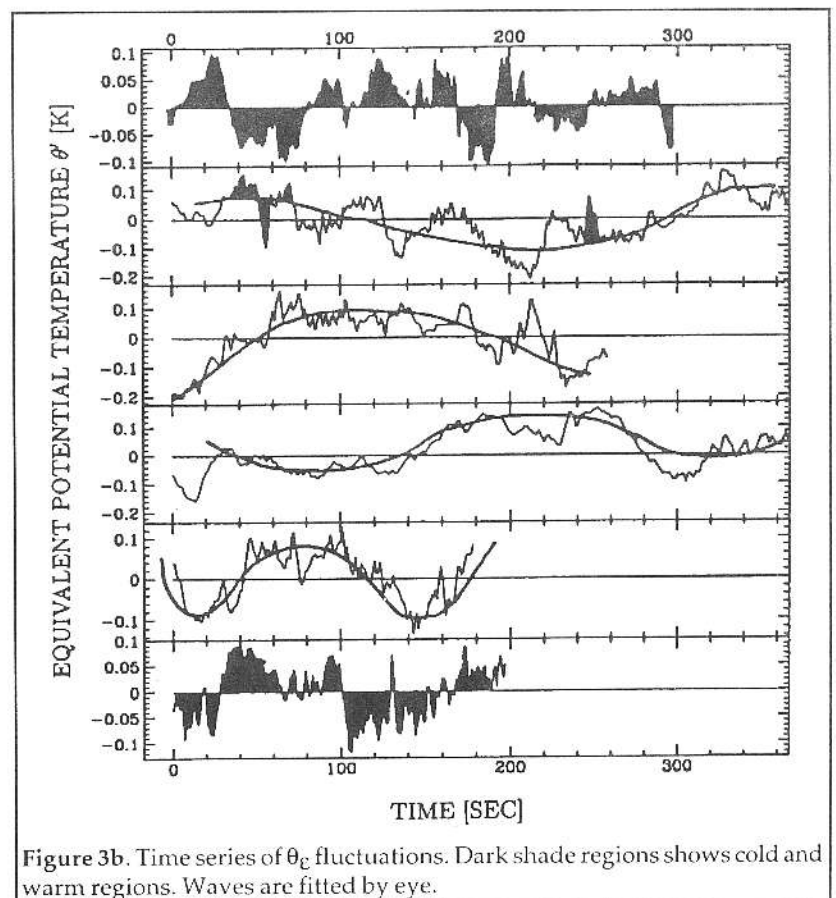
Quick change in the pitch and roll angles may cause large bias in the measurements (especially in wind components). Roll angle for S2 (sloping ascent sounding) was is almost constant (about 0 degree) during entire sounding. On the other hand, roll angle for S1(S3) varied between 9(-13) and 13(-16) degree, respectively. The significant characteristics observed in the profiles are summarized as: 1) strong inversion layer seen at about 8.2 km for S1 and S3, and it is smoothed out for S2. The profiles of horizontal wind x component U, y component V, and z component W, equivalent potential temperature θ_E and ice crystal concen-

tration N_i are shown in Figure 4. Smoothed structures are also observed below the inversion layer. Convectively unstable layers are found to be protected from smoothing in the upper levels (at about 9.2 km) and lower levels (at about 8.6 km). It was clear that soundings from spiral descents enlarge the small scale structures.

The profiles for θ_E and N_i for three soundings indicate that cirrus during its life had some clearing (see Figure 4). A strong inversion layer with 200 m thickness in the vertical was seen at about 8.7 km for S1 and S3 cases (not for S2 case). Cirrus was stable below the inversion layer and unstable above it. Embedded convection in the upper layers was indicated from the soundings. Convection and turbulence were very intense compared to those for the layer below the inversion.

4.3 Gravity waves

Gravity waves are commonly found in the upper troposphere (Einaudi, 1975). They can be generated because of vertical shear of horizontal wind, convection, or orographic effects. Jet streams regions consisted of strong temperature and wind gradients in the horizontal and vertical are



Leg	Altitude km	phenomena size km	\bar{w}'^+ m s ⁻¹	$\overline{w'^2}^+$ m s ⁻¹	\bar{w}'^- m s ⁻¹	$\overline{w'^2}^-$ m s ⁻¹	α_{TRS}	dominant process
1	7.75	$c \leq 3$	0.25	0.17	-0.34	0.28	0.61	turbulence-convection
2	8.17	$\lambda \approx 15$	0.27	0.22	-0.23	0.15	1.42	wave-turbulence
3	8.48	$\lambda \approx 15$	0.24	0.19	-0.24	0.20	0.97	turbulence-wave
4	8.80	$\lambda \approx 15$	0.42	0.24	-0.33	0.19	1.16	turbulence-wave
5	9.15	$\lambda \approx 40$	0.26	0.18	-0.24	0.19	0.97	wave-turbulence
6	9.45	$c \leq 3$	0.24	0.19	-0.32	0.27	0.72	convection-turbulence

Table 3. shows the sizes of the processes, and mean and standard deviation of positive and negative fluctuations of vertical velocity w . The α_{TRS} is the threshold parameter for cell definition. The c and λ signify the size of the cell and wave phenomena, respectively.

favorable for wave generation. As mentioned before, a strong inversion layer is observed at about 8.8 km.

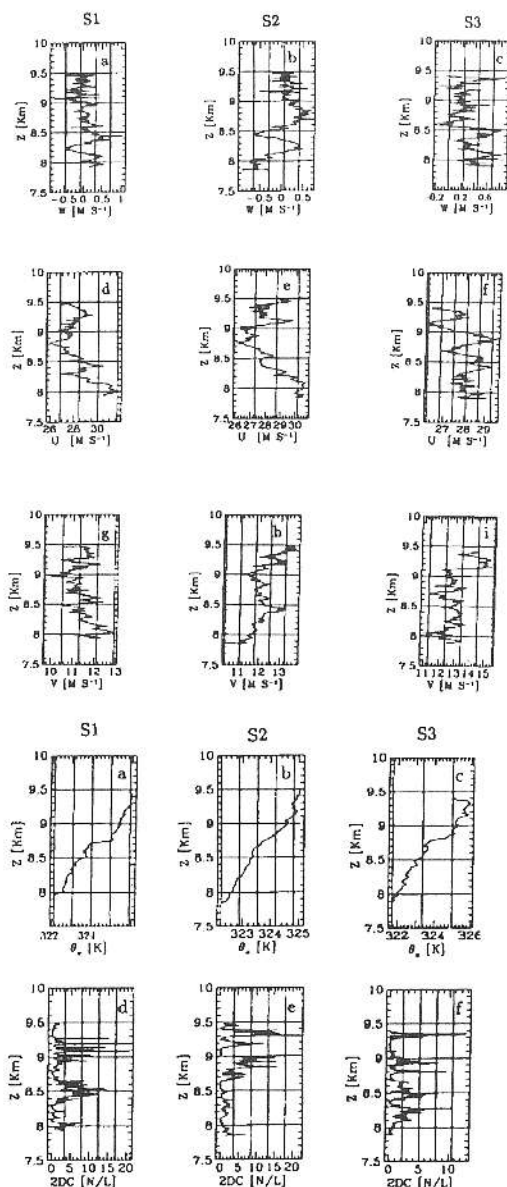


Figure 4. Profiles of θ_E , Ni , W , U , and V for soundings S1, S2, and S3.

Below this level, environment became statically stable. Above the inversion level, environment was neutrally unstable. Profiles of w (see Figure 4) showed that strong turbulent type fluctuations are observed above the inversion layer. On the other hand, wave like fluctuations are seen below the inversion layer. They are trapped in the less stable layer below the inversion and they can only propagate horizontally (Metcalf, 1975). Time series of w' in the leg 2 and 5 show the wave type of fluctuations with sizes between 15 and 40 km. Vertical propagating wave is also seen in the profile of w below the inversion layer (see Figure 4). Wave like appearance of w' is probably transformed into turbulence above the inversion layer.

4.4 Partition of turbulent heat fluxes

Partition of heat fluxes are obtained from the technique described by Grossman (1982). Heat fluxes for the constant altitude flight legs are shown in Figure 5. Meaning of each symbol (i.e., \circ , \times , \bullet , Δ) is shown in the right panel of top figure. Upward moving cells are shown by $[x]$, downward moving cells by $[°]$, entrainment (and mixing) processes by $[•]$ and $[\Delta]$. Strong entrainment processes are seen in leg 6. Convective activity (see Figures 3 and 4) is also found to be important in the same leg. In addition, entrainment processes are found to be important in the lowest flight leg although they are small compared to those for Leg 6. Heat fluxes in the convective cells are found to be much higher in the neutrally unstable environment conditions (above the inversion layer). Positive and negative values of maximum heat fluxes, and largest size of process are shown in Table 4. It is seen from this table that strong entrainment processes and cell activity occur close to the cloud top. Heat fluxes of entire cirrus for (+) and (-) values are of about -2.3 and 0.5 Kd^{-1} , respectively. These values are comparable with those obtained within the boundary layer. This explains how important turbulent heat fluxes for cirrus development in a jet stream area.

4.5 Error in the Measurements and Calculations

Error in the horizontal wind measurements can be as

Leg	Altitude km	max(+) K m s^{-1}	size (+) km	max(-) K m s^{-1}	size(-) km
1	7.75	0.04	2	0.05	5
2	8.17	0.02	2	0.04	3
3	8.48	0.04	8	0.02	2
4	8.80	0.06	1	0.15	2
5	9.15	0.04	2	0.06	2
6	9.45	0.1	2	0.2	4

Table 4. Maximum values of positive and negative heat fluxes (in $\text{m s}^{-1} \text{ K}$), and largest sizes (in km) of the structures obtained from time series of $w'\theta_E$.

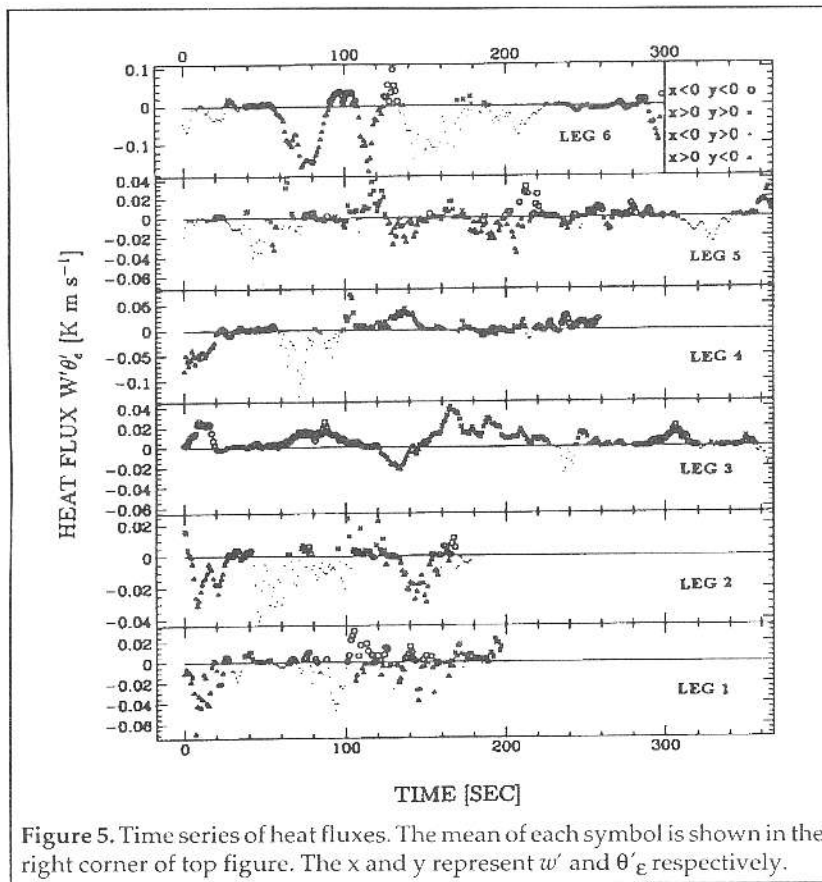


Figure 5. Time series of heat fluxes. The mean of each symbol is shown in the right corner of top figure. The x and y represent w' and θ'_ϵ respectively.

high as 1 ms^{-1} . This error depends on flight time and it increases with time. Vertical velocity measurements in a single point includes an error approximately 25 cm s^{-1} (average value for entire cirrus). In case of averaging for entire leg, the error is reduced to $10\text{--}15 \text{ cm s}^{-1}$ which is caused by deviations from attitude angles and air-speed over constant altitude flight leg (Malkus, 1953). Temperature measurements may include an error of about 0.2K (Heymsfield et al., 1990). The error in the wind fluctuations is given by Lemon (1976) of about 8% of the value of lateral wind (normal to aircraft axis) and 2% of the value of vertical velocity along the aircraft axis, down to about 10 cm s^{-1} . Error in the temperature fluctuations is approximately 0.03K (Lemon, 1976).

Error in heat fluxes is about 30%. Because of averaging over constant altitude flight leg which is about 30 km, mean fluxes may include large error (Gültepe and Starr, 1991). This type of error can only be reduced to small values, making longer constant altitude flight legs of about 60 km.

5. Conclusions

The aim of this work is to apply bivariate statistical analysis to data obtained by an aircraft from an upper tropospheric jet stream cirrus cloud. Time series and soundings from aircraft measurements are used as main data set.

Results showed that partition of heat fluxes into different sub regions are useful to indicate the regions of

turbulence and gravity wave activity. New extensive data set from FIRE II field project which took place over the Kansas region in 1992 would provide detailed information on dynamical and thermodynamical structures, and radiative processes of jet stream cirrus clouds. Data during FIRE II field project were collected from various platforms, including aircraft (with 20 Hz sampling rate), satellites, radars and lidars, and radisondes.

Acknowledgements

The author would like to thank Dr. A. J. Heymsfield of the Mesoscale and Microscale Meteorology Division of NCAR, and Dr. D. O'C Starr for discussions and comments during this study. The author would also like to thank the National Research Council (NRC) and the Climate and Radiation Branch of NASA/GSFC for funding and providing facilities to improve this manuscript.

References

- Conover, J. H., 1960: Cirrus patterns and related air motions near the jet stream as derived by photography. *J. Meteor.*, 17, 532-546.
- Holt, T. R., and S. Raman, 1992: Three dimensional mean and turbulence structure of a coastal front influenced by the gulf stream. *Mon. Wea. Rev.*, 120, 17-39.
- Gültepe, I., and D. O'C Starr, 1992: Dynamic activity, turbulence, and gravity waves within cirrus and clear air from aircraft measurements during FIRE. Submitted to *J. Atmos. Sci.*
- Gültepe, I., A. J. Heymsfield, and D. H. Lenschow, 1990: A comparison of vertical velocity in cirrus obtained from aircraft and lidar measurements during FIRE. I. *Atmos. Ocean. Tech.*, 7, 58-67.
- Grossman, R. L., 1982: An analysis of vertical velocity spectra obtained in the Bomex fair weather, trade-wind boundary layer. *Boundary Layer Meteor.*, 23, 323-357.
- Grossman, R. L., 1984: Bivariate conditional sampling of moisture flux over a tropical ocean. *J. Atmos. Sci.*, 41, 3238-3253.
- Greenhut, G. K., and J. S. Khalsa, 1982: Updraft and downdraft events in the atmospheric Boundary layer over the equatorial pacific ocean. *J. Atmos. Sci.*, 39, 1803-1817.
- Heymsfield, A. J., K. M. Miller, and J. D. Spinhirne, 1990: The 27-28 October 1986 FIRE IFO Cirrus case study: Cloud microstructure. *Mon. Wea. Rev.*, 118, 2313-2328.
- LeMone, M. A., 1983: Momentum transport by a line of cumulonimbus. *J. Atmos. Sci.*, 40, 1815-1834.
- Einaudi, F., and D. P. Lalas, 1975: Wave-induced insta-

- bilities in an atmosphere near saturation. *J. Atmos. Sci.*, 536-558.
- Malkus, J. S., 1953: Some results of a trade-cumulus cloud investigation. *J. Meteor.*, 11, 220-237.
- Metcalf, J. L., 1975: Gravity waves in a low-level inversion. *J. Atmos. Sci.*, 32, 351-361.
- Nakagawa, Y., and P. Frenzen, 1955: A theoretical and experimental study of cellular convection in rotating fluids. *Tellus*, 7, 1-21.
- Schaefer, V. J., and W. E. Hubert, 1955: A case study of jet stream clouds. *Tellus*, 3, 301-307.
- Shao, Y., J. M. Hacker, and P. Schwerdtfeger, 1991: The structure of turbulence in a coastal atmospheric boundary layer. *Q. J. R. Meteor.*, 117, 1299-1324.
- Starr, D. O'C, and D. P. Wylie, 1990: The 27-28 October 1986 FIRE cirrus case study: Meteorology and clouds. *Mon. Wea. Rev.*, 118, 2259-2287.